Effects of Adding Silver Oxide Nanoparticles to Anodized Titanium Surfaces

Renan Eduardo Reidel[a] [ID], *Sandra Raquel Kunst[a]* [ID], *Luana Góes Soares[a*]* [ID],

Fernando Dal Ponte Morisso[a] [ID], *Ana Luisa Ziulkoski[a]* [ID], *Eduardo Luís Schneider[b]* [ID],

Claudia Trindade Oliveira[a] [ID]

[a]*Universidade Feevale, Instituto de Ciências Criativas e Tecnológicas (ICCT), 93352-000, RS, Novo Hamburgo, Brasil.*

[b]*Universidade Federal do Rio Grande do Sul, Departamento de Engenharia de Materiais, Av. Bento Gonçalves, 9500, Porto Alegre, RS, Brasil.*

The present study aimed to analyze the effects of the anodization process and addition of silver nanoparticles by sealing process on corrosion resistance and biofilm formation in titanium. For this purpose, CP grade 2 titanium samples were pickled and anodized in Psidium Guajava-based electrolyte, in galvanostatic mode with the application of 0.1 mA/cm^2 for 300 s. For the incorporation of silver nanoparticles, the sealing process was used. The sealing of the anodized samples was performed in sodium carbonate solution without and with the addition of 0.25, 0.5, 1 and 2 mM AgNO$_3$, for 30 minutes at a temperature of 75 ºC. The samples were characterized regarding their morphology by Scanning Electron Microscopy (SEM), Energy-Dispersive X-ray Spectroscopy (EDS) and atomic force microscopy (AFM), corrosion resistance by potentiodynamic polarization, and bactericidal action by optical density microtiteration. The anodizing process resulted in the formation of an oxide layer (TiO$_2$), with greater surface roughness and better anticorrosive performance, compared to pure titanium. The sealing process proved to be effective for incorporating silver into the anodized titanium surface, at all concentrations evaluated, inhibiting the proliferation of Escherichia coli and Staphylococcus aureus bacteria, favoring the bactericidal effect.

Keywords: *Titanium, Silver Oxide Nanoparticles, Anodization, Escherichia coli.*

1. Introduction

Thousands of surgical procedures are performed daily to repair bone tissue damaged by fractures, infections or tumors, which makes the field of biomaterials a vital area of research, as they can improve the quality and longevity of human life[1,2].

Among biomaterials, titanium is one of the most used materials for biomedical applications due to its useful properties, such as biocompatibility and corrosion resistance. Clinically, the main challenges for titanium (Ti) implantation are bacterial infection, aseptic loosening, and elastic modulus incompatibility and corrosion, which severely affect the survival rate of implants. During dental implant surgery, for example, obtaining a completely sterile environment is difficult, as the oral cavity contains more than 600 species of bacteria, increasing the risk of infection. Another factor that makes good osseointegration difficult is the fact that, even with a high resistance rate, titanium can corrode in the presence of body fluids. Furthermore, despite its biocompatibility, studies have shown that titanium alloys do not form chemical bonds with bone tissue[2,3].

Surface treatments applied to implants have shown good results in terms of osteoblastic adhesion and osseointegration.

Among these methods, anodization is a treatment used to form an oxide layer (TiO$_2$), through electrolysis, on the titanium surface. Oxides generated by titanium anodization can be of the barrier or porous types, depending on the anodization conditions and the electrolyte used. For implants, the commercial anodization process uses an electrolyte containing HF, which is harmful to the health of the operator. As a response, new, environmentally friendly electrolytes have been tested for use in implants, such as those based on *Psidium guajava*. The resulting TiO$_2$ layer assists in the corrosion resistance process and stimulates the growth of hydroxyapatite, which is essential for the osseointegration of biomedical implants[4-6]. As for infections, the antimicrobial activity of silver oxide nanoparticles (Ag$_2$ONPs) has been shown to be effective in combating viruses, fungi and a wide spectrum of bacterial strains, in addition to having a beneficial effect on corrosion resistance. Regarding bacteria, nanoparticles can, in short, cause cell death by penetrating their cell walls[7-9].

Poor osseointegration and bacterial infections are flaws that profoundly affect the survival rate of a titanium implant. Therefore, the present study aimed to analyze the effects of the anodization process and addition of silver nanoparticles through the sealing process, on corrosion resistance and biofilm formation on titanium.

*e-mail: lugoes.soares@gmail.com

Reidel et al. *Materials Research*

2. Experimental Methods

2.1. Surface preparation

To carry out this study, first, samples of commercially pure (CP) titanium, grade 2, acquired from the Company Acnis do Brasil Steel Products Trading Ltda, were prepared, measuring 7 cm x 2.5 cm and pickled in a solution of 60% nitric acid (HNO_3) + 40% hydrofluoric acid (HF) for 10 s, immediately before the anodizing process. Afterwards, they were washed in running water and dried under a flow of cold air.

2.2. Anodizing process

The titanium samples were anodized using a voltage source of 0-300 V and current of 0-0.5 A. Each titanium sample was connected to the positive pole of the source and titanium electrodes were connected to the negative pole. The anodizations were carried out in galvanostatic mode with a current density of 0.1 mA/cm^2 applied for 300 s. Once the process was complete, the samples were washed in running water and dried under a flow of cold air[10].

2.3. Incorporation of silver nanoparticles

For the incorporation of silver oxide nanoparticles, the sealing process was used. This process was employed after anodizing it to hydrate the oxide and seal irregularities. Sealing was done with silver nitrate solutions at concentrations of 0.25, 0.5, 1 and 2 mM, using a 1% w/V sodium carbonate solution, in a proportion of 3:1. The solutions were heated to 75 ºC, then the anodized samples were immersed for 30 min. The temperature was maintained between 75 ºC and 85 ºC. Afterwards, each sample was removed from the solution, washed in running water and dried under a flow of cold air. The process was carried out for each anodized sample individually[11]. Table 1 below shows the nomenclatures used for non-anodized, anodized and sealed samples.

2.4. Characterization of titanium samples

To analyze the micrograph in a top view perspective and observe the chemical composition of the surfaces, the samples were evaluated using SEM (scanning electron microscopy)

Table 1. Shows the nomenclatures used for the non-anodized, anodized and sealed samples.

| Sample identification	Process parameters
Ti	Pure Titanium
Ti-D	Pickled Pure Titanium
Ti-A	Anodized Titanium
Ti-S	Anodized Titanium Sealed in Sodium Carbonate
Ti-A-0.25Ag	Anodized Titanium Sealed in 0.25 mM $AgNO_3$ Solution
Ti-A-0.5Ag	Anodized Titanium Sealed in 0.5 mM $AgNO_3$ Solution
Ti-A-1Ag	Anodized Titanium Sealed in 1 mM $AgNO_3$ Solution
Ti-A-2Ag	Anodized Titanium Sealed in 2 mM $AgNO_3$ Solution

and EDS (energy-dispersive X-ray spectroscopy), after metallization with a gold target to allow electrical conduction and image acquisition. AFM (atomic force microscopy) analysis was carried out with the aim of determining the roughness of the samples. For each sample, an area of 5 x 5 μm was analyzed, whose average roughness (Ra) and maximum roughness (Rmax) were evaluated. To analyze the corrosion rate of surfaces, potentiodynamic polarization was performed when in contact with inflammatory SBF (simulated body fluid), with the following composition: NaCl (8.035 g), $NaHCO_3$ (0.355 g), KCl (0.225 g), $K_2HPO_4.3H_2O$ (0.231 g), $MgCl_2.6H_2O$ (0.311 g), HCl (1.0 M) (39 mL), $CaCl_2$ (0.292 g), Na_2SO_4 (0.072 g), $(OHCH_2)_3CNH_2$ (6.118 g), and HCl (1.0 M) (2 mL) obtaining a pH = 5.5. The test used a 1 mV/s sweep starting at -200 mV and reaching +400 mV with respect to the open circuit potential. To evaluate the influence of Ag_2ONPs on the bactericidal activity of the samples, the growth of three strains of bacteria (Pseudomonas aeruginosa ATCC 27853, Escherichia coli ATCC 25922 and Staphylococcus aureus ATCC 25923) over the metallic plates are microtitration analyses were performed as previously described (Kayser et al., 2023)[12]. Briefly, samples fixed on sterile cell culture were inoculated with each strain (in independent experiments) and incubated at 36ºC for 48 h. Then, the bacterials were fixed with 4% formaldehyde and were stained with 0,4% crystal violet. The samples were washed with saline solution, and the dye were solubilized in absolute ethanol. Then, the absorbance was measured at 580 nm.

3. Results and Discussion

3.1. Morphological analysis using SEM and chemical composition analysis using EDS of titanium samples

Figure 1 shows the top-view SEM micrograph of the pure titanium (Ti) and pickled titanium (Ti-D) samples at magnifications of 1000x, 2000x and 5000x.

The presence of titanium grains can be seen in the images, Figure 1, which is in accordance with ASM (1985), which indicates the microstructure of unalloyed, high-purity, cold-rolled and annealed titanium in the form of grains. Some irregularities arising from the manufacturing of the material are also observed (yellow circle), which was also verified by[10] when using grade 2 CP titanium. The micrographs of titanium pickled in the HF+HNO_3 solution showed a structure like that of pure titanium, with fewer imperfections on the surface and the removal of the oxide layer formed on the Ti surface. Furthermore, the formation of small irregularities such as protuberances and craters (red circles) are also observed. Pickling aims to remove the thin oxide layer generated spontaneously on the titanium surface. According to[13], pickling is useful because it allows a clean surface to facilitate the application of subsequent treatments, such as anodizing or other chemical surface modification processes. Surface modification is often reported as an implant treatment that can occur in several steps, each considering a specific surface characteristic. Chemical and electrochemical treatment methods are essential especially
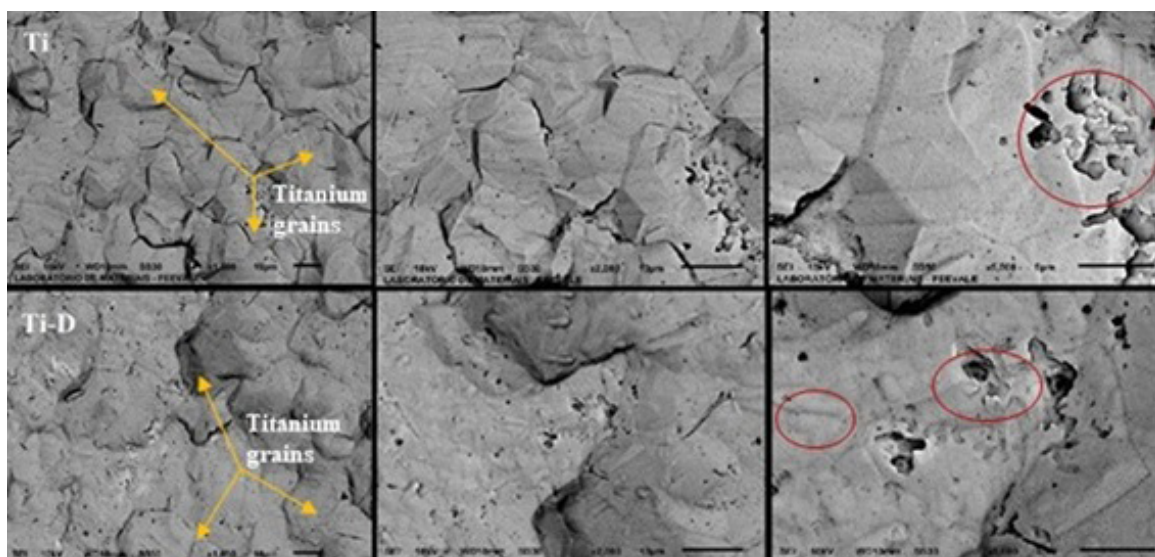
Figure 1. Top-view micrograph of the pure titanium and pickled titanium samples at magnifications of 1000x, 2000x and 5000x.

for products and implants whose complex geometry could be compromised if any other type of traditional treatment, such as mechanical polishing, were applied. The authors etched a biodegradable alloy containing Fe-13Mn-1.2C with variations in time (30 s and 60 s) and temperature (21 ºC and 60 ºC), with the acids HNO_3, HF and HCl, among others. After almost all pickling conditions were met, cavities and porous structures were observed. The authors attributed these characteristics to some residues from the previous oxide layer. Several particles were found and attributed to accidental contamination, which in the case of this work may be associated with the manufacturing process. When evaluating the surface morphology, the authors verified that not all conditions resulted in a scale removal process, providing a homogeneous final topography.

Figure 2 shows the micrograph, in a top view, of the anodized titanium surface in the *Psidium guajava*-based electrolyte.

After anodization, as shown in Figure 2, the characteristic grains of pure titanium can be observed, but with less definition than those of Figure 1. Since the morphology observed is like that of the non-anodized sample, it can be inferred that the layer of the oxide formed has a very thin thickness and is possibly of the barrier type. Studies were developed using *Psidium guajava* extract as an electrolyte in the anodization of titanium, generating barrier-type oxides. An analysis of the *Psidium guajava* electrolyte suggests the presence of species that contain phenolic groups in the electrolyte composition, in addition to the possibility that the formation of the oxide layer may be associated with the presence of such groups[10]. In Figure 2, it is possible to observe an increase in surface roughness caused by the probable formation of anodic oxide, like the results observed by[14] in titanium samples anodized in citric acid with a concentration of 15% for 5 minutes. Also verified was the formation of nanometer-sized porosity, of approximately 60 nm, in which the morphology of titanium grains was observed[15].

Although the corrosion resistance of anodized titanium is greater compared to that of natural oxide, the porous structure generated in some anodizing processes can leave the surface of the material susceptible to corrosion at some points. This factor makes it necessary to seal the pores and irregularities of the anodized oxide[16].

Figure 3 shows the micrograph, in top view, of the titanium surface anodized in a *Psidium guajava*-based electrolyte and sealed in a sodium carbonate solution.

The micrographs of the material after anodizing and sealing show the formation of irregularities (blue circle). It is observed that such irregularities on the surface of the samples appear to be formed as an "opening" of the grain boundary and may have occurred through contraction of the oxide with sealing. According to authors, at temperatures above 60 °C there is an increase in internal compression stresses in the oxide due to electrostriction. However, in the sealing process, it was expected that there would be hydration of oxide with an increase in volume, which was not seen in the SEM images[17-19].

Figure 4 shows the top-view micrograph of the anodized titanium surface after the insertion of silver oxide nanoparticles at concentrations of 0.25, 0.5, 1.0 and 2.0 mM of $AgNO_3$ by sealing.

In Figure 4, clusters of particles (blue circle) possibly containing silver oxide can be seen, indicating that the incorporation of silver occurred for all Ag concentrations in the sealing process.

However, clusters were also observed in the highest concentration of silver analyzed (Ti-A-2Ag). Di et al.[20] found that the size, distribution and quantity of silver nanoparticles are related to the concentrations of the $AgNO_3$ solution. According to the author[20], with increasing concentrations, Ag nanoparticles agglomerate, forming large clusters. For the Ti-A-1Ag sample, a more homogeneous distribution of silver was observed, compared to the other samples. This behavior can be observed in Figure 5, which shows the chemical mapping performed on the samples.
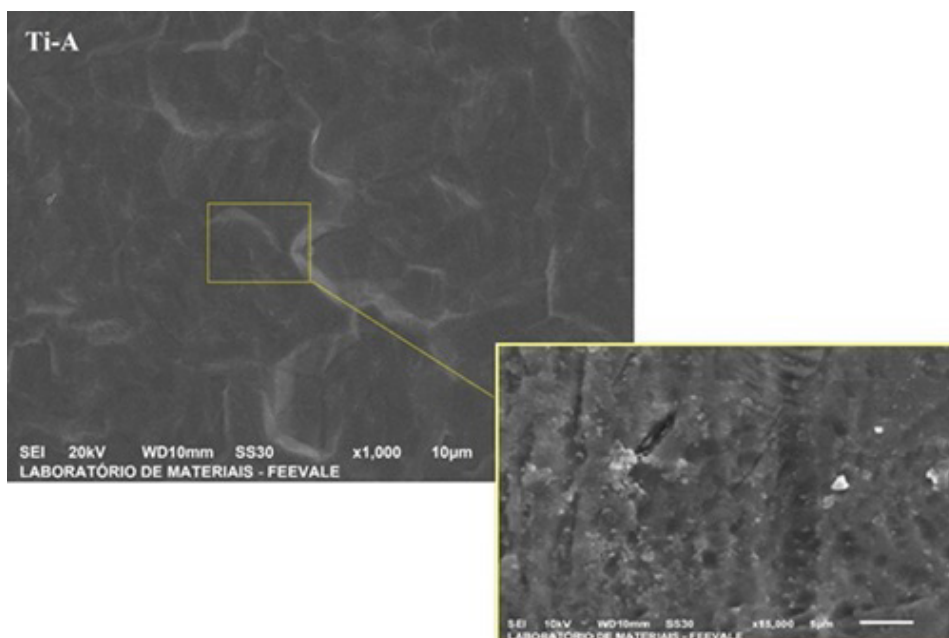
Figure 2. Micrographs obtained by top-view SEM of the titanium (Ti-A) samples anodized in *Psidium guajava*.
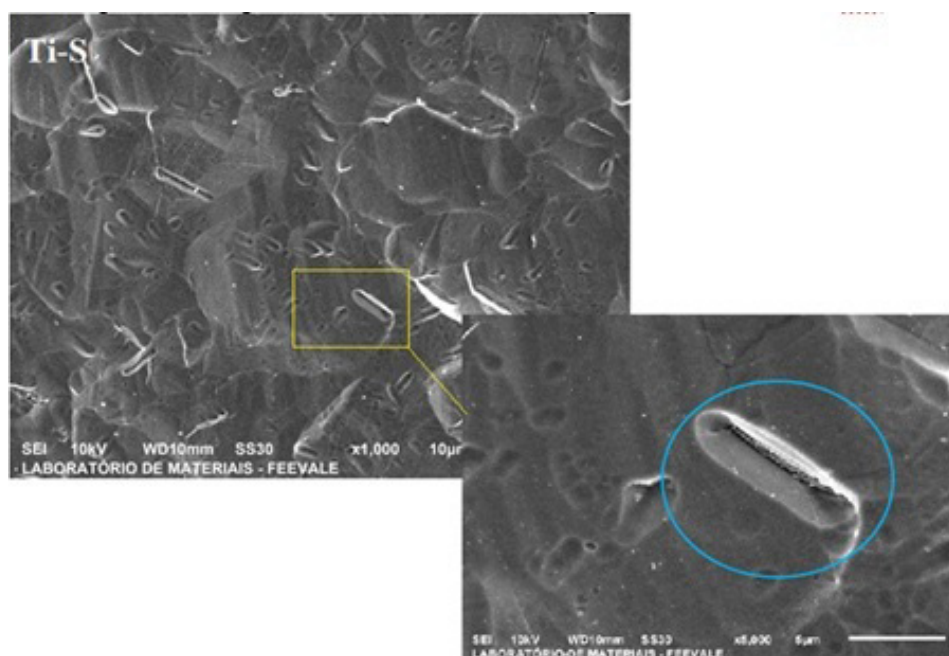
Figure 3. Micrographs obtained by top-view SEM of the titanium (Ti-S) samples.

As shown in Figure 5, silver oxide clusters are observed in some samples, indicated by yellow circles. According to[21], the greatest difficulty in the synthesis of AgNPs is obtaining stable colloidal dispersions, given that particle growth occurs through aggregation. The aggregation process occurs because AgNPs are very small and their contact surface is very large, so they cluster together to minimize the total area, forming secondary particles and reducing the interface tension of the system and the same should happen with Ag_2ONPs.

However, the Ti-A-1Ag sample was the only one that did not present silver oxide clusters, that is, better distribution of silver oxide on its surface should be obatined, corroborating the results analyzed by SEM (Figure 5-c). Di et al.[20] carried out a study on the effects of silver nanoparticles on titanium. They incorporated silver into the samples by immersion in solutions containing different concentrations of silver, namely 50, 100 and 200 mMolar $AgNO_3$. The authors found that there is an "optimal" concentration, which results in a better distribution of silver in the sample.
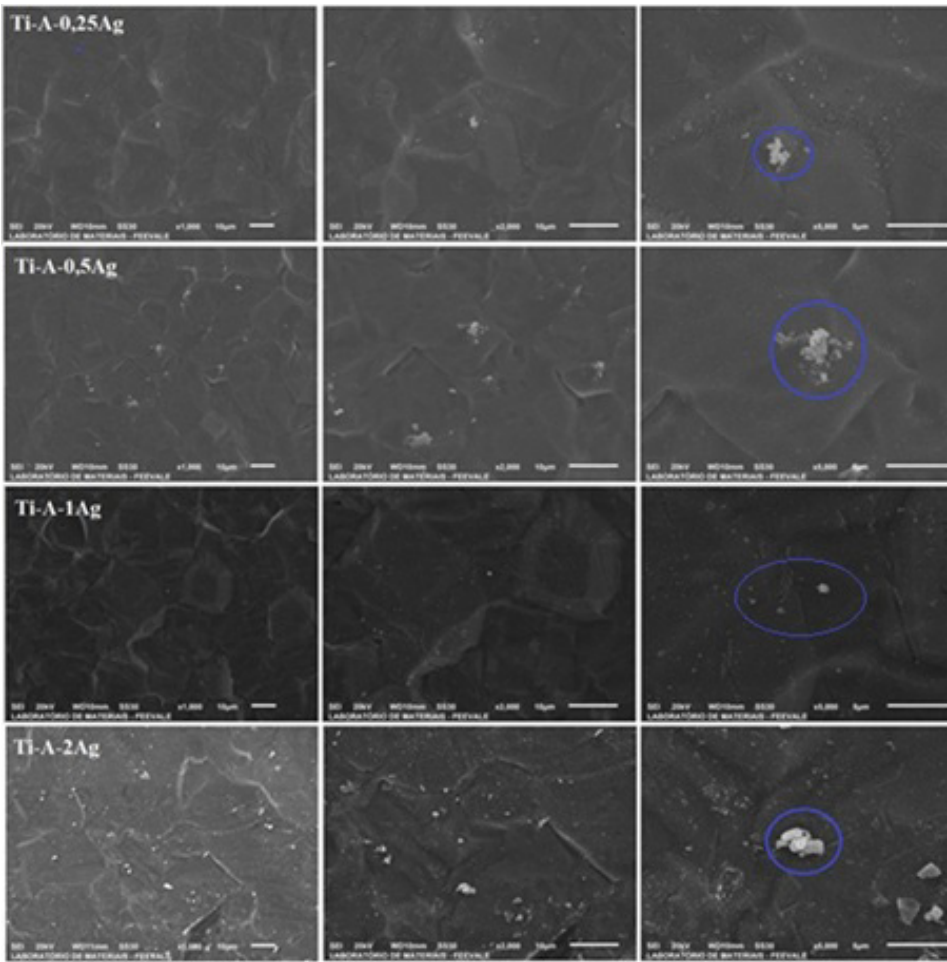
Figure 4 - Micrographs obtained by top-view SEM of the titanium samples: Ti-A-0.25Ag; Ti-A-0.5Ag; Ti-A-1Ag; Ti-A-2Ag.
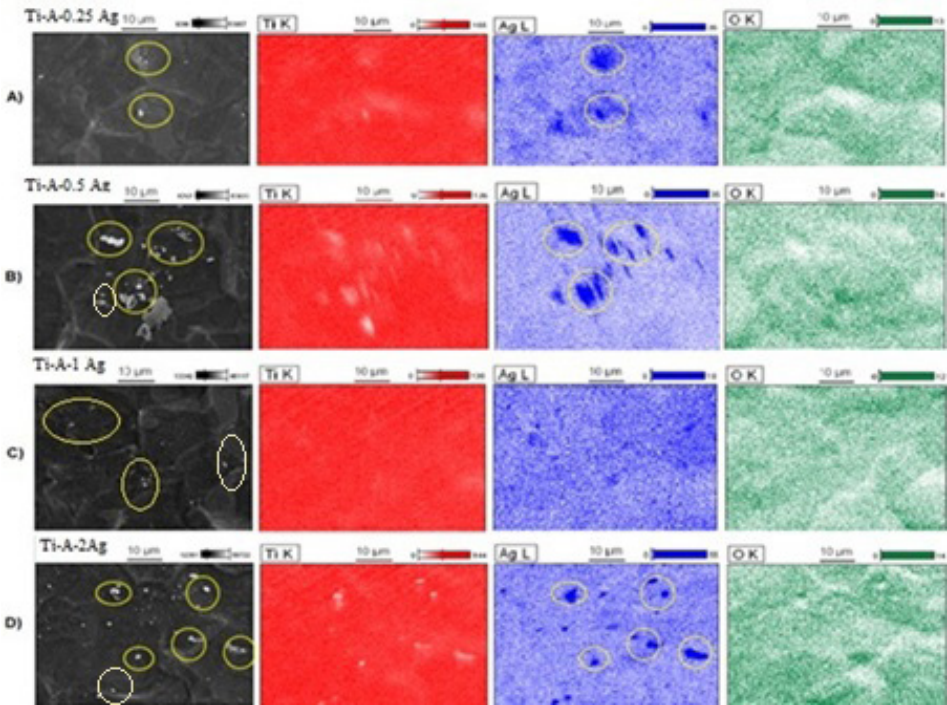

Figure 5. Chemical mapping in top view of titanium samples under the conditions: Ti-A-0.25Ag; Ti-A-0.5Ag; Ti-A-1Ag; Ti-A-2Ag.

Furthermore, it was observed that after reaching the optimal incorporation concentration (Ti-A-1Ag) on the surface, obtaining homogeneous distribution, the increase in concentration promoted the saturation of the solution, with consequent occurrence of agglomerate formation. Akhavan et al.[22] studied the photodegradation of *Escherichia coli* in the presence of an Ag-TiO$_2$/Ag/a-TiO$_2$ nanocomposite film and observed that due to saturation, the release process of silver ions may not be controlled, resulting in greater release and consequently decreasing its electrochemical performance, causing the contamination of the human body with silver residues.

3.2. AFM (atomic force microscope)

All biomaterials intended for bioactive applications must have complex topographical features. Surface features in the nanometer range play an important role in protein adsorption and cell attachment. In Figure 6, the variation in the surface behavior of titanium samples without and with treatment can be observed using AFM (atomic force microscopy).

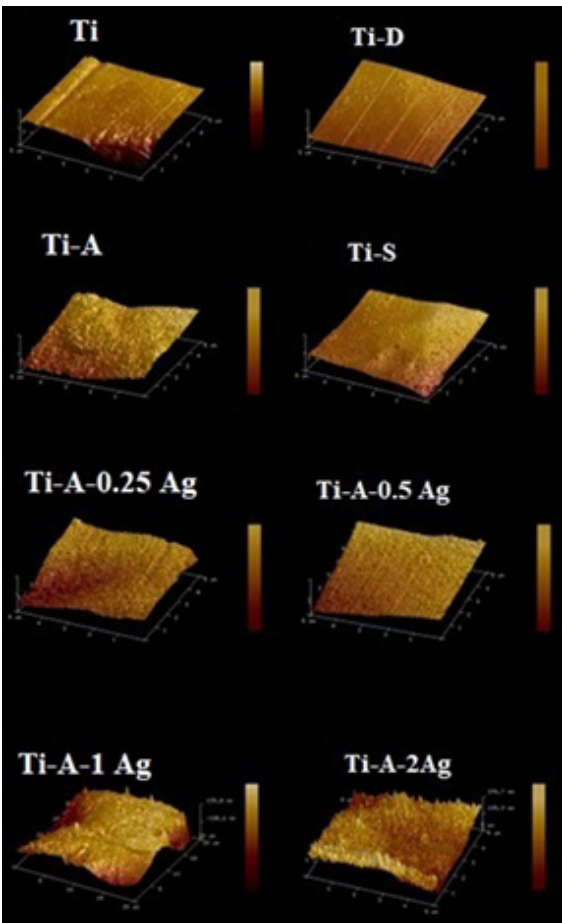Table 2 presents the Ra (average roughness) and Rmax (maximum roughness) data obtained using AFM.

According to Figure 6, the pure titanium sample shows irregularities on its surface, which are related to the sheet manufacturing process as analyzed in Figure 1, based on the SEM analysis. However, with the data presented in Table 2, a decrease in the Ra of pure titanium is observed, compared to samples coated with silver nanoparticles and using the anodization process. Studies have evaluated the surface of grade 2 pure titanium and observed that the surface roughness of this material is uniform and regular[6].

Regarding the pickled sample, it has a smoother appearance compared to pure titanium. This behavior was already expected, since pickling cleans dirt and oxides, removing the natural oxide layer from the titanium. According to the study carried out by[23], pure pickled titanium has a roughness of around 13.7 ± 4.0 nm.

The anodized sample has an apparently rougher surface compared to the pickled one, which indicates the formation of an oxide on the titanium surface. Although the SEM analyses show a morphology very similar to that of the non-anodized sample (Figure 2), with a very thin oxide layer, AFM analysis confirms that the anodization led to the formation of an oxide and a rough surface. Some authors point out that surface roughness can interfere with the behavior of materials in the face of corrosive processes. Generally, the higher the surface roughness parameter of a system, i.e. the rougher it is, the lower its resistance to corrosion, since surface roughness increases the contact area of the coating with solutions that cause chemical attack. In the case of biomaterials, body fluids can cause attack, accelerating the corrosion process that may occur and initially deteriorating the surface of the substrate[24,25].

Studies mention that the electrochemical potential of a metallic implant varies depending on the roughness of its surface; therefore, a rougher surface offers less restriction for electrons to be released, resulting in a lower electrochemical potential[26].

According to[27], titanium, compared to other biomaterials, has low surface roughness. Using anodization, topographically

Figure 6. Atomic force microscopy of the samples (Ti; Ti-D; Ti-A; Ti-S; Ti-A-0.25mM; Ti-A-0.5mM; Ti-A-1mM; Ti-A- 2mM).

Table 2. Ra (average roughness) and Rmax (maximum roughness) values obtained by AFM.

Samples	Ra (nm)
Ti	25.9
Ti-D	13.5
Ti-A	37.1
Ti- S	26
Ti-A-0.25 Ag	44.8
Ti-A-0.5 Ag	32.9
Ti-A-1Ag	92.5
Ti-A-2Ag	-

complex surfaces can be obtained at micro and nanometric levels. It has been demonstrated that the nanometric texture produced by anodization provides an efficient means to improve the attachment and proliferation of proteins and osteoblastic cells, which are well-known parameters for cellular response in the early phase of osseointegration[3,28].

The sealed sample, on the other hand, showed lower roughness (Ra = 26 nm) compared to anodized titanium (Ra = 37.1 nm). It is known that sealing promotes oxide hydration, thus the sealing treatment of the Ti-S sample reduced the roughness of the anode coating, sealing the microstructural defects and leveling the surface. Although the SEM analyses

carried out (Figure 3) showed the formation of irregularities on the surface of the samples, the data obtained by AFM had the expected characteristics after sealing, making it possible to observe the reduction in average roughness and the leveling of the surface caused by the hydration of the oxide[17].

In samples in which silver was incorporated, there was a tendency for roughness to increase with rising Ag surface concentrations. Kayani et al.[29], studied the effects of adding different concentrations of silver to zinc oxide (ZnO) prepared using the sol-gel process. The authors[29] observed that increasing silver concentrations generated surface agglomerates of Ag and increased the surface roughness of the samples[29]. Studies also evaluated the behavior of coating based on polydimethylsiloxane (PDMS) and silver phosphate (Ag_3PO_4) nanocomposites at 1, 3, 5 and 7% by weight of Ag_3PO_4 in relation to PDMS. The authors noted that the surface became rougher with increasing silver concentrations, reaching the point of forming Ag clusters in the 7% by weight coatings. As the silver concentration increases, the nanoparticles find it easier to adhere to each other, forming an interconnected and compact structure on the surface of the coating. The agglomeration of nanoparticles in the surface layer leads to the creation of cavities and grooves, reducing the solid/liquid contact area[30].

Based on Table 2, the average roughness (Ra) and maximum roughness (Rmax) show an increasing trend with rising silver concentrations, although in a discreetly in the case of the and Ti-A-0.5Ag, when compared to Ti-A and Ti-S samples. The Ti-A-1Ag sample had a roughness of 92.5 nm, which was significantly greater than the roughness of anodized titanium and the Ti-A-2 Ag sample. This value made data collection impossible due to the maximum roughness detection limit of the AFM equipment. These results indicate that higher concentrations of $AgNO_3$ make surfaces rougher.

Greater roughness undermines protection against corrosive processes; however, when it comes to biomaterials, greater roughness allows for better biocompatibility. A smooth surface, without roughness, does not allow good biocompatibility, since the integration of implants into bone tissue *in vivo* is related to an increase in the roughness of the implant surface. This is due to the fact that human osteoblasts adhere better to rough surfaces[31,32].

3.3. Polarization

Figure 7 shows the graph of the potentiodynamic polarization curves of samples a) Ti; Ti-A; Ti-D and b) Ti-S; Ti-A-0.25Ag; Ti-A-0.5Ag; Ti-A-1Ag; Ti-A-2Ag and immersed in SBF solution.

Based on the potentiodynamic polarization curves obtained in the SBF electrolyte (Figure 7a), it was observed that the Ti, Ti-A and Ti-D samples showed similar behavior, with fluctuations in the corrosion potential at values close to 0 V (zero volts), and corrosion current density values of approximately 10^{-8} A/cm^2. However, Ti showed an abrupt increase in current density in the active region, indicated by charge transfer. Studies[33] have shown that titanium spontaneously passives in solutions with a low concentration of fluoride ions. However, when the concentration of fluoride ions is greater than 0.002 M, the potentiodynamic polarization curves of titanium show multiple corrosion potentials and an increased anode current. This is due to the

Samples	Ra (nm)
Ti	25.9
Ti-D	13.5
Ti-A	37.1
Ti- S	26
Ti-A-0.25 Ag	44.8
Ti-A-0.5 Ag	32.9
Ti-A-1Ag	92.5
Ti-A-2Ag	-

Figure 7. Polarization in samples a) Ti; Ti-A; Ti-D and b) Ti-S; Ti-A-0.25Ag; Ti-A-0.5Ag; Ti-A-1Ag; Ti-A-2Ag and immersed in SBF solution.

attack and degradation of the passive titanium film by the fluoride ion. This behavior is also observed in other halides, such as the Cl$^-$ ion.

In the case of this work, the oscillations observed in the corrosion potential, as well as the increase in the anodic current, related to charge transfer, are possibly linked to the presence of chloride in the SBF electrolyte. Furthermore, the Ti, Ti-A and Ti-D samples show an increase in their anodic current density after charge transfer, which is indicated by a passivation process. It is worth noting that the passivation regions also show oscillations, which are more intense in the Ti curve, like pits. Titanium has the characteristic of valve metal and therefore spontaneously passives to form a compact passive film that covers the entire surface, avoiding contact with the corrosive medium. Typically, once the passive film is damaged, it immediately recovers. However, the passive behavior of titanium is affected by some factors such as the corrosive environment to which it is exposed.

According to studies[34], Cl$^-$ attack promotes the dissolution of passive films. A higher density of oxygen vacancies is produced in the passive film because of the insertion of Cl$^-$, resulting in pitting corrosion. According to the author, the Cl$^-$ adsorbed on the surface of the sample would permeate the passive film and be trapped by oxygen vacancies. Because of charge compensation, more oxygen vacancies would be generated. Such associations would result in the formation of voids (pitting nucleation). Therefore, a high density of oxygen vacancies in the passive film would ultimately result in increased corrosion.

Furthermore, it is observed that the corrosion current density limit of Ti is ($\sim7x10^{-7}$) A/cm^2, approximately one order of magnitude higher compared to Ti-A and Ti-D ($\sim7x10^{-8}$) A/cm^2, as shown in Figure 7. In this case, although Ti forms oxides spontaneously in air, it is possible that this oxide has been damaged and recovered over time, resulting in an oxide with surface defects. However, regarding the Ti-D sample, the resulting oxide was removed and its complete formation, possibly with fewer surface defects (originating from the rupture and oxide coating), Figure 1, resembling the anodized sample.

Furthermore, comparing the Ti-D sample with Ti-A, it is observed that Ti-D has more oscillations in its passive region. Pickling aims to remove the thin oxide layer spontaneously generated on the titanium surface, thus increasing biocompatibility and corrosion resistance. However, titanium can corrode in the presence of body fluids, which contain organic and inorganic ions and molecules capable of breaking the protective oxide barrier and damaging the material. In this case, the layer of titanium oxide (TiO_2) generated during anodizing helps in the corrosion resistance process, as oxygen not only functions as a corrosion stimulator, but can also act to a certain extent as a protector, reacting with the metal surface and forming a protective layer capable of delaying contact between the metal and the corrosive environment[5,6].

According to studies[35], for potentials greater than 6 V or temperatures over 60 °C, the electric field applied during anodization exerts electrostriction (mechanical deformation in a dielectric that follows the direction of the electric field), leading to internal compression stresses in the resulting oxide. This indicates that the oxide formed by anodization is thicker or denser than that formed in air.

Comparing the anodized sample, Ti-A (Figure 7a), with the sealed sample, Ti-S (Figure 7b), a small shift in potential to more noble values is observed, toward approximately 100 mV. Furthermore, the corrosion current density increases approximately 1 order of magnitude. This can be explained due to the tensions generated in the oxide during sealing, which caused openings to appear in the grain boundary. These imperfections would be responsible for the higher corrosion current density.

According to Figure 7b, the corrosion potential value shifted to more noble values with the increase in silver concentration in Ti-A-0.25Ag, Ti-A-0.5Ag, Ti-A-1Ag and Ti-A-2Ag. This may have occurred due to the uniform and compact deposition of silver on the surface, which would make the access of corrosive agents difficult.
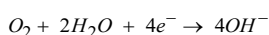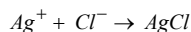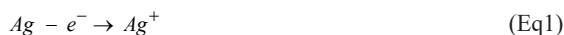
It is observed that all sealed samples, with and without silver, showed corrosion current density of the same order of magnitude. Ti-A-0.25Ag has a current density peak in the active region indicated by charge transfer, like Ti (Figure 7a). After that, the current density drops and stabilizes, in a process of passivation, followed by a new peak, and becomes passive again, followed by another peak. This observed current density peak behavior may be related to pitting. In the other samples containing silver, an abrupt increase in current density in the active region is also observed, followed by oscillations in current density and peaks related to pitting. However, in sealed titanium, pitting is not observed.

In a study[36] carried out with AgCu and AgCuTi alloys immersed in SBF solution, it was found that the silver concentration decreases, and the Cl concentration gradually increases with immersion time. The authors[36] relate this process to a continuous deposition-dissolution reaction. For the AgCu alloy, there was dissolution of silver and copper. For the AgCuTi alloy, only silver dissolved. The authors justified this behavior due to Cu forming a solid solution with Ti. In this case, the Ti in the AgCuTi alloy hardly dissolves and precipitates, ensuring that the solid solution effect inhibits damage to surrounding body tissues. In this study, it was observed that titanium presented electrochemical behavior like that of the AgCuTi alloy, which can be observed in the passivation regions.
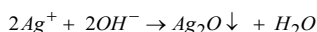
The authors[36] describe that the silver atom is released in the SBF solution, in the form of Ag+, reacting with Cl- to generate a AgCl precipitate. Electrons generated during silver oxidation combine with the oxygen dissolved in the SBF solution to form OH-. The corrosive process can be described according to Equation 1.

Dissolution process:

$$Ag - e^- \rightarrow Ag^+ \tag{Eq1}$$

$$Ag^+ + Cl^- \rightarrow AgCl$$

$$O_2 + 2H_2O + 4e^- \rightarrow 4OH^-$$

Deposition:

$$2Ag^+ + 2OH^- \rightarrow Ag_2O\downarrow + H_2O$$

The authors found that the deposition process was dominant in relation to the dissolution process. In the present study, the pits observed may be related to the reaction of silver with chlorine, forming silver precipitates. However, it is observed that, despite the occurrence of pitting, the increase in silver concentration shifts the corrosion potential to more noble values. Authors found that the presence of silver increases corrosion resistance and helps maintain antibacterial activity for long periods of immersion in SBF, which means that in real situations, silver reduces the probability of prosthesis rejection[36,37].

3.4. Assessment of bactericidal action on titanium samples

The results of the biofilm formation assessment of the samples Ti, Ti-A, Ti-D, Ti-S, Ti-A-0.25Ag, Ti-A-0.5Ag, Ti-A-1Ag and Ti-A-2Ag against *Pseudomonas aeruginosa*, *Escherichia coli* and *Staphylococcus aureus* are shown in Figure 8.

In the data presented in Figure 8, a progressive reduction in absorbance was observed against *Pseudomonas aeruginosa*, indicating a reduction in the formation of biofilms with an increase in the concentration of $AgNO_3$. However, these results did not indicate a beneficial effect when compared to samples without silver on their surface. *Pseudomonas aeruginosa* has, as one of its defense mechanisms, low membrane permeability, as the bacillus limits the entry of antibiotics by altering its transport proteins such as porins, for example[38]. This causes the efflux of antibiotics to occur outside the cell, preventing them from accumulating in the cytoplasm of the bacterial cell[39].

Authors[39] studied the bactericidal effect of silver nanoparticles, demonstrating that these nanoparticles are efficient bactericidal agents for *Escherichia coli*. In the present study, against *Escherichia coli*, samples containing silver showed better performance compared to samples without silver on the surface, with the best result being that of Ti-A-2Ag surfaces, which had an average abs/cm^2 in the range of 0.066. This behavior was also observed with *Staphylococcus aureus*, where the best performances among all samples were those of Ti-A-1Ag surfaces, with an average abs/cm2 of 0.07 (standard deviation 0.0120),
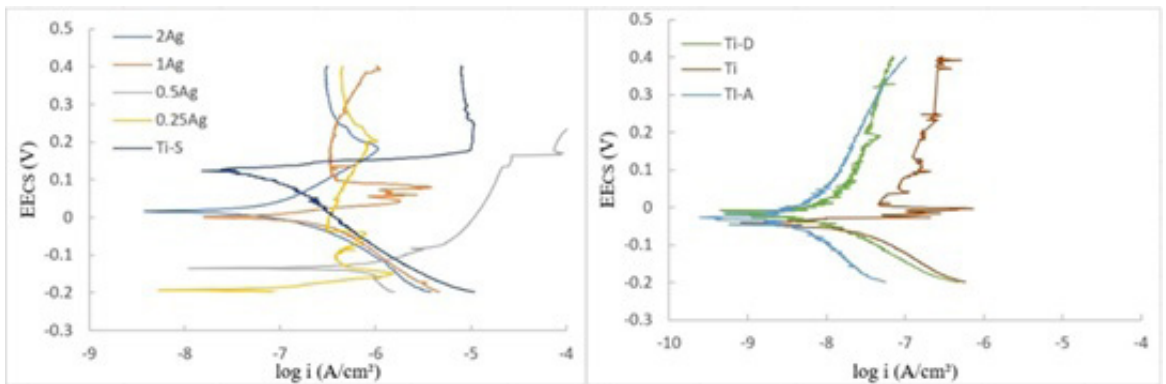
Figure 8. Assessment of biofilm formation of samples Ti, Ti-A, Ti-D, Ti-S, Ti-A-0.25Ag, Ti-A-0.5Ag, Ti-A-1Ag and Ti-A-2Ag against *Pseudomonas aeruginosa*, *Escherichia coli* and *Staphylococcus aureus*.

and Ti-A- 2Ag surfaces, with an average abs/cm^2 of 0.068 (standard deviation 0.02).

Silver nanoparticles can cause cell death by penetrating bacterial cell walls. In addition to its nanoscale size, high surface-area- to-volume ratio, the ability to release ions and free radicals contribute to its effectiveness[7,8]. In the present study, it was found that the incorporation of silver nanoparticles favored the inhibition of biofilm growth for *Escherichia coli* and *Pseudomonas aeruginosa*. When evaluating Figure 8, it is evident that the Ti-A-2Ag sample obtained the best performance, as it offered greater resistance against the development of biofilms among the samples containing silver. Therefore, it can be stated that increasing the concentration of silver on the surface increases the inhibition of biofilm growth.

4. Conclusions

The present study aimed to analyze the effects of the anodization process and addition of silver nanoparticles through the sealing process, on corrosion resistance and biofilm formation on titanium. Based on the results obtained, it can be concluded that: The anodizing process in the *Psidium guajava*-based electrolyte resulted in a thin oxide layer (TiO$_2$), which increased surface roughness and had better anti-corrosion performance compared to pure titanium. The sealing process resulted in the formation of pits on the surface of the samples, with an "opening" appearance of the grain boundary, which was attributed to the contraction of the oxide. However, as observed via AFM, sealing resulted in oxide hydration, which was seen in the reduction of surface roughness. The sealing process proved to be effective for incorporating silver into the anodized titanium surface in all concentrations evaluated, and there is a specific concentration of silver dissolved in the sealing solution, in which the deposition occurs more homogeneously. This concentration varies according to the methodology used. Increasing the concentration of silver in the sealing solution tends to increase the concentration of silver on the surface and the surface roughness of the material, in addition to shifting the corrosion potential to more noble values. Analyses of the biofilm formation inhibition test for *Escherichia coli* and *Staphylococcus aureus* indicated that the incorporation of silver by sealing, in anodized samples, favored the bactericidal effect, showing an increase in inhibition with an increase in silver concentration.

5. Acknowledgments

6. References

1. Asri RIM, Harun WW, Samykano M, Lah NAC, Ghani SAC, Tarlochan F, et al. Corrosion and surface modification on biocompatible metals: a review. Mater Sci Eng C. 2017;77:1261-74. http://doi.org/10.1016/j.msec.2017.04.102.

2. Lin R, Wang Z, Li Z, Gu L. A two-phase and long-lasting multi-antibacterial coating enables titanium biomaterials to prevent implants-related infections. Mater Today Bio. 2022;15:100330. http://doi.org/10.1016/j.mtbio.2022.100330.

3. Nouri A, Shirvan AR, Li Y, Wen C. Surface modification of additively manufactured metallic biomaterials with active antipathogenic properties. Smart Materials In Manufacturing. 2023;1:100-001. http://doi.org/10.1016/j.smmf.2022.100001.

4. Ronoh K, Mwema F, Dabees S, Sobola D. Advances in sustainable grinding of different types of the titanium biomaterials for medical applications: a review. Biomedical Engineering Advances. 2022;4:100-047. http://doi.org/10.1016/j.bea.2022.100047.

5. Tsuchiya H, Macak JM, Müller L, Kunze J, Müller F, Greil P, et al. Hydroxyapatite growth on anodic TiO$_2$ nanotubes. J Biomed Mater Res A. 2006;77(3):534-41. http://doi.org/10.1002/jbm.a.30677.

6. Kunst SR, Cerveira DO, Ferreira JZ, Graef TF, Santana JÁ, Carone CLP, et al. Influence of simulated body fluid (normal and inflammatory) on corrosion resistance of anodized titanium. Research. Soc Dev. 2021;10(10):1-26. http://doi.org/10.33448/rsd-v10i10.18606.

7. Rahmah MI. Study the effect of graphene and silver nanoparticles on the structural, morphological, optical, and antibacterial properties of commercial titanium oxide. Inorg Chem Commun. 2023;149:1. http://doi.org/10.1016/j.inoche.2023.110441.

8. Gunputh UF, Le H, Handy RD, Tredwin C. Anodised TiO$_2$ nanotubes as a scaffold for antibacterial silver nanoparticles on titanium implants. Mater Sci Eng C. 2018;91:638-44. http://doi.org/10.1016/j.msec.2018.05.074.

9. Fernandes M, Kunst SR, Morisso FP, Carús LA, Ziulkoski AL, Oliveira CT. Inserção de nanocargas de prata em superfície de titânio anodizado. Research. Soc Dev. 2022;11(7):1-19. http://doi.org/10.33448/rsd-v10i10.18606.

10. Cerveira DO, Kunst SR, Mueller LT, Morisso FP, Ziulkoski AL, Cauduro R, et al. Titanium Anodization in Psidium Guajava. Research. Soc Dev. 2022;11(12):1-25. http://doi.org/10.33448/rsd-v11i12.34953.

11. Pornnumpa N, Jariyaboon M. Antibacterial and corrosion resistance properties of anodized AA6061 aluminum alloy. Eng J (NY). 2019;23(4):171-81. http://doi.org/10.4186/ej.2019.23.4.171.

12. Kayser CKC, Mueller LT, Soares LG, Volz DR, Ziulkoski AL, Schneider EL, et al. Organic-inorganic films with anticorrosive and bactericidal properties for titanium implants. Mater Res. 2023;26:e20230218. http://doi.org/10.1590/1980-5373-mr-2023-0218.

13. Andrade LM, Paternoster C, Chevallier P, Gambaro S, Mengucci P, Mantovani D. Surface processing for iron-based degradable alloys: a preliminary study on the importance of acid pickling. Bioact Mater. 2022;11:66-180. http://doi.org/10.1016/j.bioactmat.2021.09.026.

14. Kieser TA, Kunst SR, Morisso FP, Machado TC, Oliveira CT. Anodização de titânio em ácido cítrico. Research. Soc Dev. 2022;11(8):1-18. http://doi.org/10.33448/rsd-v11i8.30872.

15. Kunst SR, Graef TF, Mueller LT, Morisso FDP, Carone CLP, Fuhr LT, et al. Superficial treatment by anodization in order to obtain titanium oxide nanotubes applicable in implantology. Materia (Rio J). 2020;25(4):e25311830872. http://doi.org/10.1590/s1517-707620200004.1173.

16. Song D, Ma M, Zhao L. Study of sealing of anodized aluminium in mixed titanium-cerium salt solutions. Int J Electrochem Sci. 2022;17(12):221224. http://doi.org/10.20964/2022.12.23.

17. Liu L, Wu L, Chen X, Sun D, Chen Y, Zhang G, et al. Enhanced protective coatings on Ti-10V-2Fe-3Al alloy through anodizing and post-sealing with layered double hydroxides. J Mater Sci Technol. 2020;37:104-13. http://doi.org/10.1016/j.jmst.2019.07.032.

18. Shibata T, Zhu YC. The effect of film formation conditions on the structure and composition of anodic oxide films on titanium. Corros Sci. 1995;37(2):253-70. https://doi.org/10.1016/0010-938X(94)00133-Q.

19. Sondi I, Salopek SB. Silver nanoparticles as antimicrobial agent: a case study on e. coli as a model for gram-negative bacteria. J Colloid Interface Sci. 2004;275(1):177-82. http://doi.org/10.1016/j.jcis.2004.02.012. PMid:15158396.

20. Di H, Qiaoxia L, Yujie Z, Jingxuan L, Yan W, Yinchun H, et al. Ag nanoparticles incorporated tannic acid/nanoapatite composite coating on Ti implant surfaces for enhancement of antibacterial and antioxidant properties. Surf Coat Tech. 2020;399:126169. http://doi.org/10.1016/j.surfcoat.2020.126169.

21. Mulvaney P. Metal nanoparticles: double layers, optical properties, and electrochemistry. In: Klabunde KJ, editor. Nanoscale materials in chemistry. Hoboken: Wiley; 2001. p. 121-68. http://doi.org/10.1002/0471220620.ch5.

22. Akhavan O. Lasting antibacterial activities of Ag–TiO₂/Ag/a-TiO₂ nanocomposite thin film photocatalysts under solar light irradiation. J Colloid Interface Sci. 2009;336(1):117-24. http://doi.org/10.1016/j.jcis.2009.03.018. PMid:19394952.

23. Casagrande RB, Kunst SR, Beltrami LVR, Aguzzoli C, Brandalise RN, Malfatti CF. Pretreatment effect of the pure titanium surface on hybrid coating adhesion based on tetraethoxysilane and methyltriethoxysilane. J Coat Technol Res. 2018;15(5):1089-106. http://doi.org/10.1007/s11998-017-0035-2.

24. Brooks EK, Brooks RP, Ehrensberger MT. Effects of simulated inflammation on the corrosion of 316L stainless steel. Mater Sci Eng C. 2017;71:200-5. http://doi.org/10.1016/j.msec.2016.10.012.

25. Demarch A, Waterkemper A, Pasini D, Ruzza S, Montedo ORK, Angioletto E. Effects of roughness parameters on slip resistance for different methods used to determine the coefficient of friction for ceramic floor tiles. Ceram Int. 2021;47(17):24281-6. http://doi.org/10.1016/j.ceramint.2021.05.139.

26. Zhang XF, Liu ZG, Shen W, Gurunathan S. Silver Nanoparticles: synthesis, characterization, properties, applications, and therapeutic approaches. Int J Mol Sci. 2016;17(9):1534. http://doi.org/10.3390/ijms17091534.

27. Covani U, Marconcini S, Galassini G, Cornelini R, Santini S, Barone A. Connective tissue graft used as a biologic barrier to cover an immediate implant. J Periodontol. 2007;78(8):1644-9. http://doi.org/10.1902/jop.2007.060461.

28. Bayram C, Demirbilek M, Yalçđn E, Bozkurt M, Doğan M, Denkbaş Emir B. Osteoblast response on co-modified titanium surfaces via anodization and electrospinning. Appl Surf Sci. 2014;288:143-8. http://doi.org/10.1016/j.apsusc.2013.09.168.

29. Kayani ZN, Anwar M, Saddiqe Z, Riaz S, Naseem S. Biological and optical properties of sol–gel derived ZnO using different percentages of silver contentes. Colloids Surf B Biointerfaces. 2018;171:383-90. http://doi.org/10.1016/j.colsurfb.2018.07.055.

30. Seyfi J, Goodarzi V, Wurm FR, Shojaei S, Jafari NM, Najmoddin N, et al. Developing antibacterial superhydrophobic coatings based on polydimethylsiloxane/silver phosphate nanocomposites: assessment of surface morphology, roughness and chemistry. Prog Org Coat. 2020;149:105944. http://doi.org/10.1016/j.porgcoat.2020.105944.

31. Anderson JA, Lamichhane S, Mani G. Macrophage responses to 316L stainless steel and cobalt chromium alloys with different surface topographies. J Biomed Mater Res A. 2016;104(11):2658-72. http://doi.org/10.1002/jbm.a.35808.

32. Pfeiffer F, Herzog B, Kern D, Scheideler L, Geis G, Jürgen WH. Cell reactions to microstructured implant surfaces. Microelectron Eng. 2003;67(68):913-22. http://doi.org/10.1016/S0167-9317(03)00154-0.

33. Yang Z, Yu MH, Chao Z, Zhenjiang JIA, Xuejiao Z, Li M, et al. Jianhua. Evolution and corrosion resistance of passive film with polarization potential on Ti-5Al-5Mo-5V-1Fe-1Cr alloy in simulated marine environments. Corros Sci. 2023;221:111334. http://doi.org/10.1016/j.corsci.2023.111334.

34. Cui YW, Chen LY, Chu YHZ, Lina LR, Lu SW, Liqiang Z, et al. Metastable pitting corrosion behavior and characteristics of passive film of laser powder bed fusion produced Ti–6Al–4V in NaCl solutions with different concentrations. Corros Sci. 2023;215:111017. http://doi.org/10.1016/j.corsci.2023.111017.

35. Shibata T, Zhu YC. The effect of film formation conditions on the structure and composition of anodic oxide films on titanium. Corros Sci. 1995;37(2):253-70. http://doi.org/10.1016/0010-938X(94)00133-Q.

36. Liu B, Yan Y, Lin J, Cao J, Qi J. Corrosion behavior of Ag-based alloy in simulated body fluid solution. Vacuum. 2022;197:110850. http://doi.org/10.1016/j.vacuum.2021.110850.

37. Mazare A, Anghel A, Surdu B, Totea C, Demetrescu G, Ioana ID. Silver doped diamond-like carbon antibacterial and corrosion resistance coatings on titanium. Thin Solid Films. 2018;657:16-23. http://doi.org/10.1016/j.tsf.2018.04.036.

38. Mesaros N, Nordmann P, Plésiat P, Roussel DM, Van EJ, Glupczynski Y, et al. Pseudomonas aeruginosa: resistance and therapeutic options at the turn of the new millennium. Clin Microbiol Infect. 2007;13(6):560-78. http://doi.org/10.1111/j.1469-0691.2007.01681.x.

39. Koneman EW. Koneman texto e atlas, diagnóstico microbiológico. 6th ed. Rio de Janeiro: Guanabara Koogan; 2012.